Modelling Pulse Magnetic Welding Processes – An Empirical Approach

E. Uhlmann[1], A. Ziefle[1]

[1] Institut für Werkzeugmaschinen und Fabrikbetrieb (IWF), Technische Universität Berlin, Germany

Abstract

In recent years pulse magnetic welding technology gained an ever increasing attention. The process was known for over 40 years, yet the poor knowledge of process parameters as well as the difficulties concerning the calculability of the process due to lack of adequate software, performance and appropriate material models hindered the application of the technology. In the past, some simulations treating the process of explosive welding were conducted. There, the assumption was made to define a friction condition to the boundary regions which was reasonable due to similar conditions in the collision region during the process. However, at pulse magnetic welding processes, the contact forces are highly transient and have big gradients over the geometry.

In this paper a new empirical approach is presented, which gives the possibility of modelling the welding process by parameter-controlled bonding at the welding interface. The pulse magnetic forming process was simulated by loose coupling of electromagnetic and mechanical FEM software with the commercial code ANSYS. As geometry the joining of a duct with an internally positioned conical bolt was chosen. The material used for both duct and bolt was EN AW 6063. First of all the influences of heat generation were analyzed. Therefore, the additional thermal simulation was coupled with the electromagnetic and the mechanical simulation. The heat generation caused by the plastic deformation was considered. As the resulting temperatures were below the melting temperature of the material, further simulations were carried out without thermal simulation. In order to calibrate the welding model, a set of relevant parameters were defined. It included the cumulative plastic work, the plastic deformation in collision direction, the normal and the tangential components of the collision velocity and the collision angle between the two parts. By comparing the simulation with experiments carried out at the same specific process parameters, it was possible to reduce the set of parameters to the normal collision velocity and plastic deformation. Based on their distribution, the parameter control of the bonding condition could be adjusted. Further experiments gave a high accordance to the simulations carried out with the parameters found for this model.

Keywords

Finite element method (FEM), pulse magnetic welding, parameter controlled bonding

1   Introduction

The process of pulse magnetic welding was already applied in the 1970s [1], when it was used for solid state welds between the fuel pin cladding and a tapered end plug insert. However, the poor knowledge of process parameters as well as the difficulties concerning the calculability of the process due to lack of adequate software, computing performance and appropriate material models hindered a wide acceptance for applications of the technology. Recently, the development of software as well as hardware made sufficient progress which capacitates to model shock-forming processes. Regarding explosive welding, some simulations treating the process of explosive welding were conducted by Akbari-Moussavi. There, the assumption was made to define a friction condition to the boundary of the joining regions which was reasonable due to similar conditions in the collision region during the process [2]. Though the forming process and the pressure distribution were modelled, no information was obtained whether welding occurred nor where it occurred. The aim of the investigations in this paper is to provide a method in order to be able to predict welding as well as the location during pulse magnetic welding processes, validated by experiments.

2   Experiments

The geometry chosen for the experiments was a tube of 1mm thickness and an outer diameter of 18 mm and a bolt with a conical join-region using an angel of 4°, as can be seen in Figure 1.
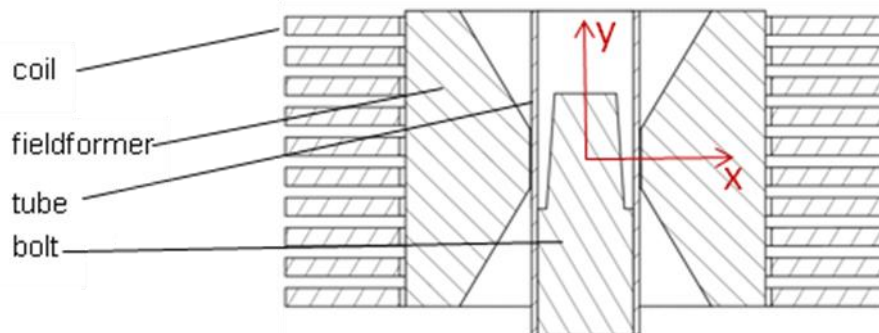

Figure 1: *Description of the Setup*

To guarantee a sufficient welding result, the tube needs a certain distance in order to sufficiently accelerate. Therefore a gap of 2 mm was set between the tube and the beginning of the cone. By pulse magnetic forming the tube was compressed and clashed on the conically turned surface. The chosen material was the aluminium alloy EN AW 6063, which properties are shown in Table 1.

Property	Value
specific resistance ρ	3,3 10^{-8} Ω m
thermal conductivity λ	201 W m^{-1}K^{-1}
specific heat capacity C_W	898 J kg^{-1} K^{-1}
thermal expansion coefficient α_W	23,5 10^{-6} K^{-1}

permeability μ	1 μ_0 = 1,2566 10^{-6} H m^{-1}

Table 1: Material properties of EN AW 6063

The experiments were carried out with a pulse magnetic forming machine (ELMAG), using a capacity of C = 240 µF with a loading voltage of U = 7,6 kV to 9,1 kV which equals a discharge energy of E_{EL} = 7 kJ to 9 kJ. The inductance of the machine for the used configuration is L_i = 0,36 µH, and the inductance of the coil is L_{coil} = 1,930 µH. This parameters of the RLC-circuit lead to a frequency of f = 7,3 kHz. For the experiments, a coil with 10 windings was used together with a fieldformer.

3   Simulations

3.1   Sequential Coupling of Electrodynamic and Mechanical FEM

The forming process is driven by the Lorentz force, which is generated due to inducted currents in the workpiece. According to [3] the skin effect has to be considered for high-frequency currents. In dependence of the conductivity of the material and the frequency of the discharge, the current experiences more resistance, the more it penetrates the material. Therefore the skindepth d is defined as:

$$d = \frac{1}{\sqrt{\kappa \mu \pi f}}$$
(1)

It is the length towards the inside direction of the material at which the current is reduced to 36 %. In this equation κ is the electrical conductivity, μ the permeability of the conductive material and f the frequency of the current. For the carried out experiments the skindepth can be calculated to d = 1,07 mm. Taking this into account, it can be assumed, that the current generating the Lorentz forces is flowing only at the outer surface of the tube. Thereby, the concept of the magnetic pressure applied to the surface of the tube can be developed. Together with the assumption, that at the inside of the workpiece the magnetic flux density is neglectable, the magnetic pressure p_{MAG} can be calculated for tubes [4]:

$$p_{MAG} = \frac{B^2}{2\mu}$$
(2)

where B is the magnetic flux density. The magnetic flux density is highly dependent on the geometry and additionally transient. At the beginning of the forming process, the tube acts like a faraday cage, forcing the magnetic flux in the gap between tube and coil. As soon as the shape of the tube is being compressed, the flux is much less concentrated, which leads to a significant drop of the magnetic pressure. Whereas in previous publications a loose coupled approach was used [5], a sequential coupled simulation model is now necessary in order to involve the change of geometry in the calculation of the Lorentz force. At the conducted simulations this was achieved by use of ANSYS APDL.

3.2 Empirical Model

Explosive welding and pulse magnetic welding are very similar concerning the bonding process [6]. It is common agreement that the welding process works as follows: a collider sheet metal plate clashes onto another plate with the inclination of the collision angle α. Due to the sudden shear strain at the collision point high pressures are generated. Therefore the material within the collision point switches to a quasi-viscous state and a material jet is generated, heading towards the free angle between the two workpieces and moving with the collision point, see Figure 2.
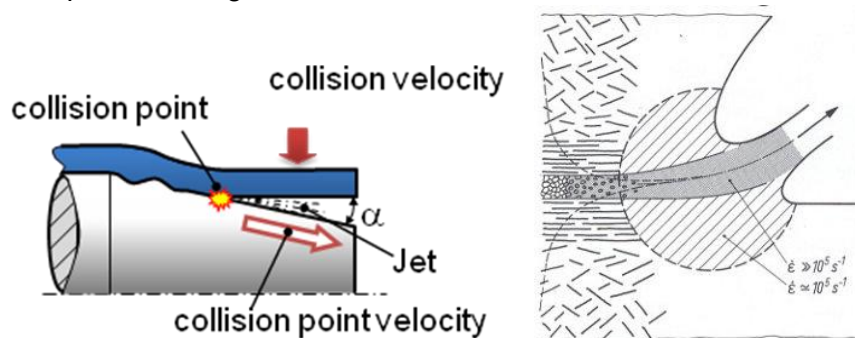

Figure 2: Welding process (left), formation of Jet (right, [7])

This way it is possible to form a thin interface layer of a few micros thick between the two workpieces. Kreye et al [7] and Koch [8] state, that the two materials approach to molecular distance and build intergranular bounds. Nevertheless the influence of the temperature should not be completely neglected. The wavy bounding structures found at experiments with pulse magnetic welding as well as explosion welding near the welding interface are comparable. Though the bounding process works similarly, there are differences between the two processes: Due to the high burning velocities of the explosives, the pressures as well as the collision velocities are usually higher than by use of pulse magnetic welding. Also, at pulse magnetic welding there is neither similar pressure nor similar deformation over the geometry of the tube. The whole welding process involves phase changes, chemical interaction and friction. A correct implementation of all effects would be either very complicated or entirely impossible due to lack of measurement data. In order to determine where welding effectively took place, a contact model has to be designed, which involves all relevant physical parameters dependent on which the contact elements will bond or continue having friction. In the literature, the weldability is very often set into relation to the collision angle, the collision velocity and the collision point velocity [5], because these parameters are measurable in experiments. As conclusion a model was implemented that can apply bonding at contact elements depending on the defined parameters.

$$B_{Bond} = f(\alpha, v_{\perp}, v_{cp}, P_{PL}, \varepsilon) \tag{3}$$

In this model B_{Bond} is a Boolean type with 1 equals to bonded and 0 equals to not bonded, α is the inclination-angle, $v_{\perp}$ the collision point velocity, v_{cp} the collision velocity, P_{PL} is the plastic work and ε is the deformation. The model does not consider cracking. After an element was bonded, it cannot be loosened any more.

3.3   Influence of the Temperature

As earlier stated, the influence of the heat generation also needs some consideration. In order to determine the influence of the heat generation due to plastic deformation and joule heating, the thermal simulation was additionally carried out after each time step of the sequentially coupled electrodynamic-mechanical simulation, sharing the same geometry. Due to the very thin welding region, the grid needed to be meshed especially in the contact region with a significantly higher definition, which led to a considerably longer calculation.

Figure 3 shows the temperature development at the inner side of the tube during the welding process. It can be seen, that the temperature never rises above 350 K, which is approximately 38 % of the melting temperature and 8 % of the required temperature difference. According to simulations the heat generated by friction, deformation and joule heating have a low influence on the welding process, the simulation of the heat generation was neglected for the further simulations.
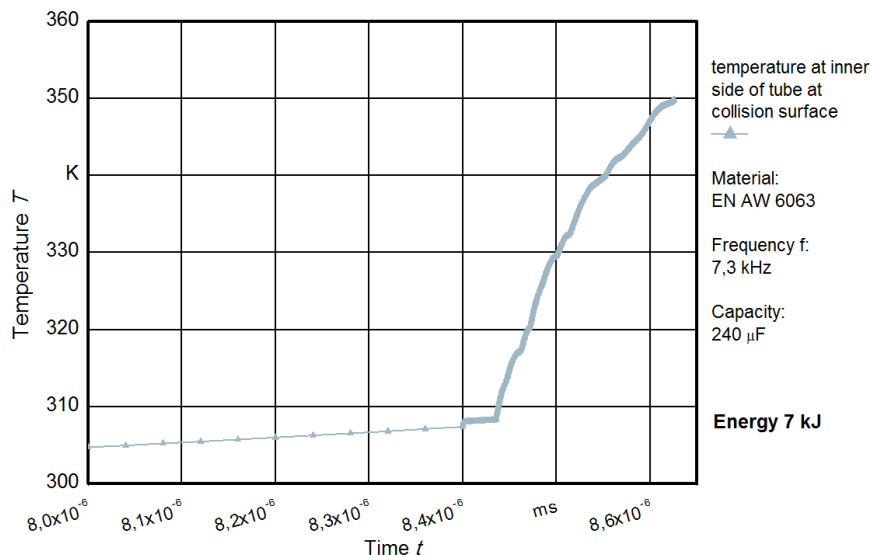

Figure 3: *Diagram of simulated Temperature of a contact element at the inner side of the tube*

4   Model setup

As a next step, the generic welding model had to be calibrated. Therefore, experiments with the later mentioned configuration were carried out, using 7 kJ and 9 kJ. At the same time simulations with the same parameters were carried out. In the interface region, a friction boundary was used. In Figure 4 the measured and simulated currents are plotted against each time for the case of 8 kJ. Though the simulation ended before the time the current had its first peak due to overdeformed elements in the bonding zone, the forming process was almost completed at this time, see Figure 5.
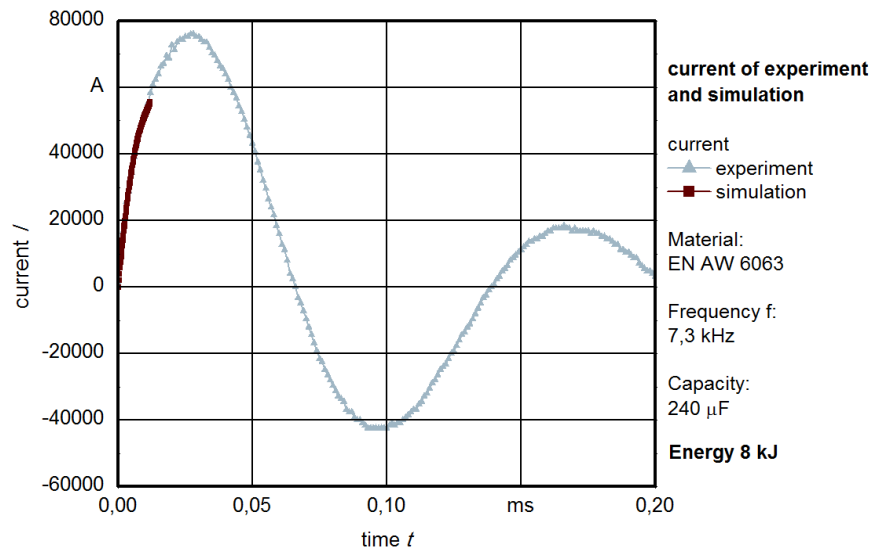
Figure 4: *Current distribution of the electromagnetic simulation and measurement*

In Figures 6 a.) to g.) each in Equation (3) defined entity is plotted over the y-coordinate of the joining zone at collision time. The collision time is the time when a node of an element of the tube collides with the surface of the bolt. As the collision is a gradual process, the collision time varies for every element. Origin and direction of the y-coordinate can be seen in Figure 1. Due to the impact of the collision there can be observed some instabilities and oscillations in the diagrams. For better data, in some cases also the diagrams of the same entities four time steps before to one time step behind the collision time are shown. The welded domains drawn as hatched areas into Figures 6 a.) to g.) show the geometrical y-position of the welds in the analogical carried out experiments. Therefore the welded probes were cut axially and polished.
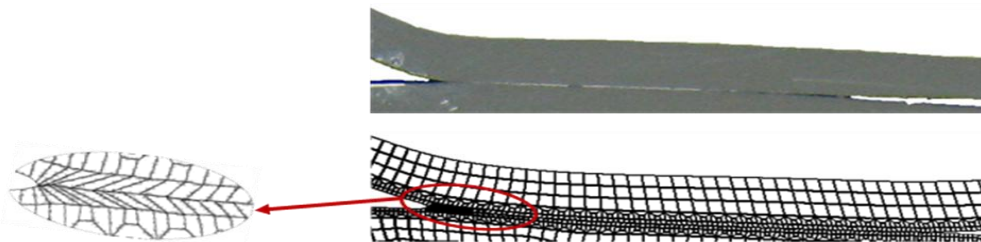

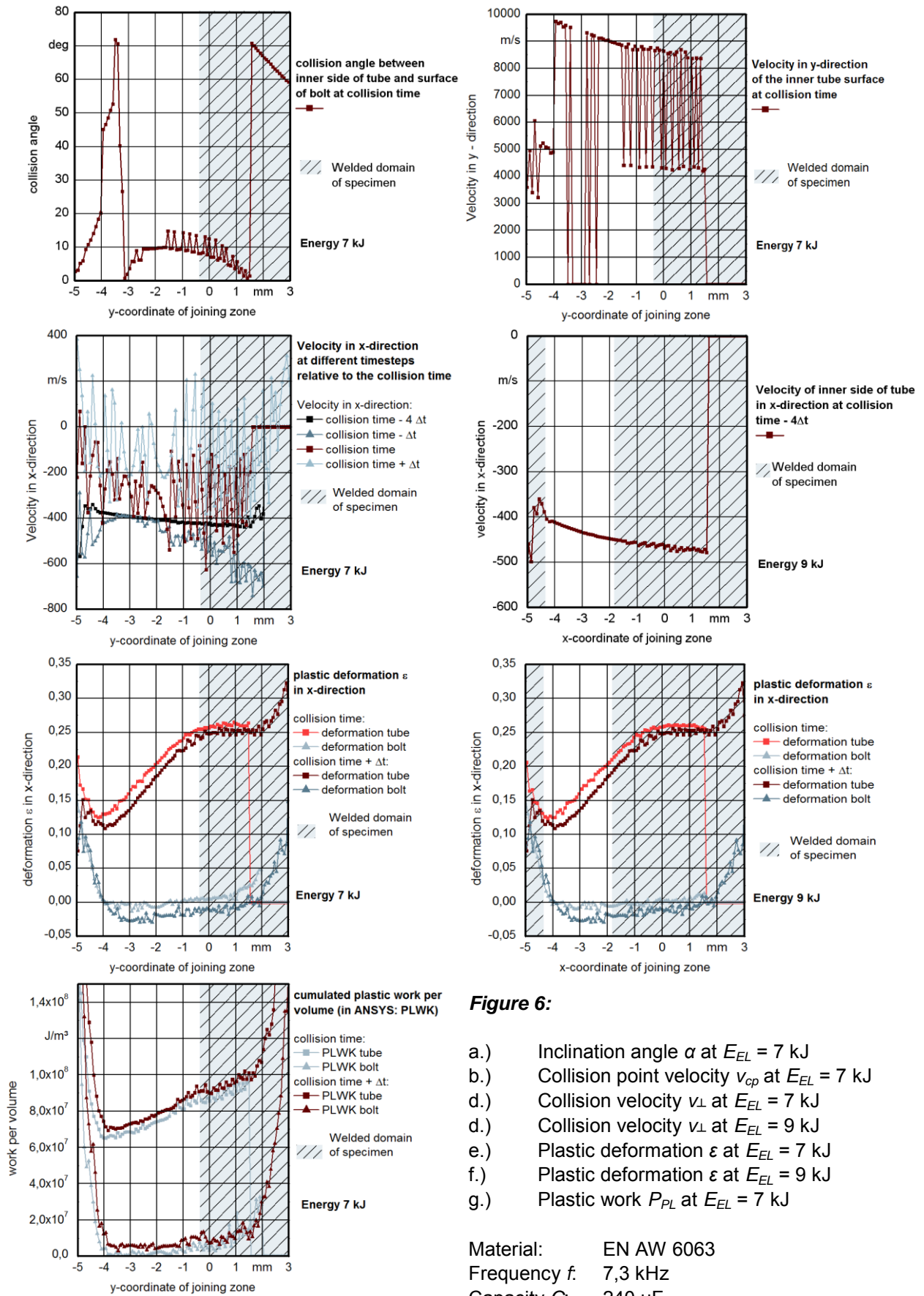
Figure 5: *Deformation of elements in the bonding region*

113

collision angle between inner side of tube and surface of bolt at collision time

Welded domain of specimen

Energy 7 kJ

Velocity in y-direction of the inner tube surface at collision time

Welded domain of specimen

Energy 7 kJ

Velocity in x-direction at different timesteps relative to the collision time

Velocity in x-direction:
— collision time - 4 Δt
— collision time - Δt
— collision time
— collision time + Δt

Welded domain of specimen

Energy 7 kJ

Velocity of inner side of tube in x-direction at collision time - 4Δt

Welded domain of specimen

Energy 9 kJ

plastic deformation ε in x-direction

collision time:
— deformation tube
— deformation bolt
collision time + Δt:
— deformation tube
— deformation bolt

Welded domain of specimen

Energy 7 kJ

plastic deformation ε in x-direction

collision time:
— deformation tube
— deformation bolt
collision time + Δt:
— deformation tube
— deformation bolt

Welded domain of specimen

Energy 9 kJ

cumulated plastic work per volume (in ANSYS: PLWK)

collision time:
— PLWK tube
— PLWK bolt
collision time + Δt:
— PLWK tube
— PLWK bolt

Welded domain of specimen

Energy 7 kJ

Figure 6:

a.)   Inclination angle α at E_{EL} = 7 kJ
b.)   Collision point velocity v_{cp} at E_{EL} = 7 kJ
d.)   Collision velocity $v_\perp$ at E_{EL} = 7 kJ
d.)   Collision velocity $v_\perp$ at E_{EL} = 9 kJ
e.)   Plastic deformation ε at E_{EL} = 7 kJ
f.)   Plastic deformation ε at E_{EL} = 9 kJ
g.)   Plastic work P_{PL} at E_{EL} = 7 kJ

Material: EN AW 6063
Frequency *f*:   7,3 kHz
Capacity *C*:   240 µF

Figures 6 a.), b.), c.) and g.) show that the data of the entities inclination-angle *α*, plastic work P_{PL}, and collision point velocity v_{cp} cannot be used for the model due to difficulties to obtain a stable course of the values. In Figures 6 e.) and f.) the plastic deforma-

114

tion of the tube with a loading energy of 7 kJ (left) and 9 kJ (right) is shown. The diagrams are quite stable over the y-axis at both energies. Also, there are only little oscillations in the graph. Unfortunately this is not the case for Figure 6 g.), where especially at the transition between welded and not welded zone oscillations of the plastic work occur. However the diagrams show that the deformation alone is not sufficient to describe welding. Therefore, the collision velocity was selected as an additional parameter. In Figures 6 c.) the collision velocity is plotted at several time steps relatively to the collision time. It can be seen that the courses at collision time, as well as one time step before and after it, are not smooth due to shockwaves induced by the impact earlier. However, using the course four time steps before collision time gives a smooth curve in the relevant region, see Figures 6 c.) and d.). It is shown, that welding can only occur after surpassing a decent particular value of collision velocity. The big step on the left side is due to the ending of the simulation, because the elements couldn't bear the steep deformations occurring at the boundary. As a result there have been defined two thresholds that have to be surpassed in order to enable welding at contact, namely a deformation of $\varepsilon = 0{,}2$ and a collision velocity of $v_\perp$ 420 m/s.

5 Results

For validation an additional simulation was carried out by use of the values obtained in the model setup with a discharge energy of $E_{EL} = 8$ kJ. In Figure 7 the results of the simulation were compared with the experimental results. The weld domain measured in a corresponding experiment is in high accordance with the weld domain in the simulation.
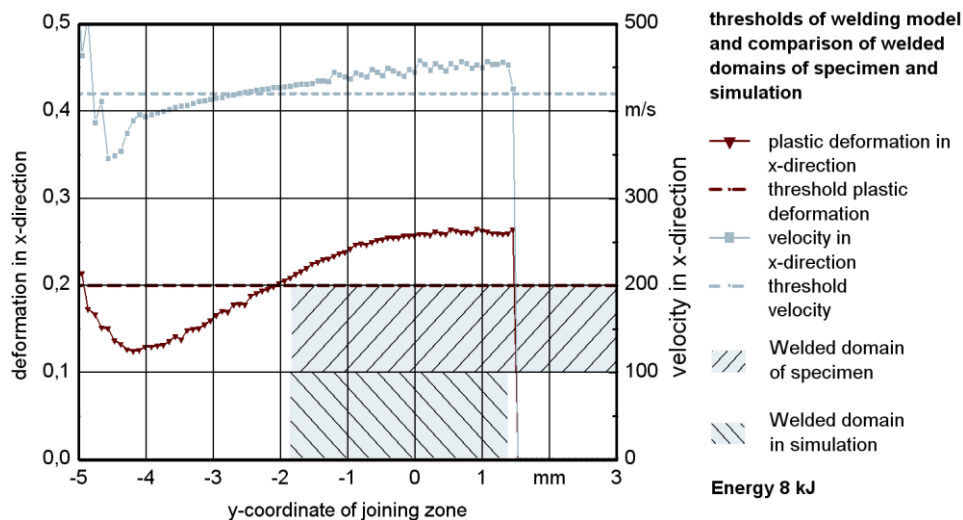

Figure 7: *Comparison of welded domains in model and simulation at $E_{EL} = 8$ kJ*

6 Conclusions

In order to model the process of pulse magnetic welding a fully sequential coupled simulation incorporating thermal, electrodynamic and structural simulation was implemented. Thereby the Lornetzforces could be directly calculated with the magnetic flux density, which includes all geometry related effects. Considering the material heating due to plastic deformation and joule heating the simulation showed low influences. Therefore the simula-

tion of thermal effects was neglected for the further cases. By comparing the simulation with experiments carried out at the same specific process parameters, the set of parameters was reduced, leaving the collision velocity and plastic deformation. Based on their distribution, the parameter control of the bonding condition could be adjusted. The validation experiment carried out using a discharge energy of 8 kJ gave a high accordance to the simulations carried out with the parameters found for this model. With this paper an empirical approach was presented to help determine the location of welds produced at pulse magnetic welding by means of simulation. Nevertheless it must be pointed out, that the found thresholds are only valid for the used material as well as the used rotational symmetric geometry. Further validation is necessary in order to expand the extent of validity as well as the usability for additional materials. Furthermore, the used model-parameters can not be obtained through experiments but only by the combination of simulations and experiments. Loosening and Cracks were not part of the Model either, not taking into account rebound effects.

References

[1] *Brown, W.; Bandas, J.; Olson, N.:* Pulsed Magnetic Welding of Breeder Reactor Fuel Pin End Closures. Reprinted from Welding Journal, June 1978.

[2] *Akbari-Mousavi, S.A.A.; Barrett, L.M.; Al-Hassani, S.T.S.:* Explosive welding of metal plates. Journal of Materials Processing Technology 202, 2008, p.224-239

[3] *Winkler, R.:* Hochgeschwindigkeitsbearbeitung – Grundlagen und technische Anwendung elektrisch erzeugter Schockwellen und Impulsmagnetfelder. VEB-Verlag Technik, Berlin, 1973.

[4] *Hahn, R.:* Werkzeuge zum impulsmagnetischen Warmfügen von Profilen aus Aluminium- und Magnesiumlegierungen. Dissertation, Uhlmann, E.(Editor) Berichte aus dem Produktionstechnischen Zentrum Berlin, 2004

[5] *Ziefle ,A.; Uhlmann, E.:* Lösungsansätze zur Darstellung des impulsmagnetischen Schweißprozesses mittels gekoppelter FEM – Simulation. Proceedings of Berliner Runde 2009.

[6] *Cramer, H.; Zech, F.; Appel, L.:* Metallographic Investigation of MPW Interfaces. Proceedings of "The first technical Conference on Industrialized Magnetic Pulse Welding & Forming", Munich, 2008

[7] *Kreye, H.; Hammerschmidt, M.; Granz, U.; Woidneck, C.-P.:* Über den Bindemechanismus beim Explosivschweißen. Schweißen und Schneiden 37, vol. 7, 1985, p 297-302.

[8] *Koch, W.:* Vorgänge beim Explosivschweißen metallischer Werkstoffe. Dissertation, Fakultät für Bergbau und Hüttenwesen der Rheinisch-Westfälischen Technischen Hochschule Aachen, 1965.